SGP-TR-93-42

PROCEEDINGS
ELEVENTH WORKSHOP
GEOTHERMAL RESERVOIR ENGINEERING

January 21-23, 1986

Henry J. Ramey, Jr., Paul Kruger, Frank G. Miller,
Roland N. Horne, William E. Brigham,
and John R. Counsil
Stanford Geothermal Program
Workshop Report SGP-TR-84*

*Sponsored by the Geothermal and Hydropower Technologies Division of the U.S. Department of Energy, Stanford-DOE Contract No. DE-AS03-80SF11459 and Contract No. DE-AS07-84ID12529

DISCLAIMER

PROCEEDINGS, Eleventh Workshop on Geothermal Reservoir Engineering
Stanford University, Stanford, California, January 21-23, 1986
SGP-TR-93

EVALUATION OF POROUS MEDIUM PERMEABILITY BY ACOUSTIC LOGGING FINDS GEOTHERMAL APPLICATIONS

B. CONCHE (1), F. LEBRETON (2), J. ROJAS (3)

(1) IPG - Institut de Physique du Globe de Strasbourg
(2) IFP - Institut Français du Pétrole, Rueil-Malmaison
(3) BRGM - Bureau de Recherches Géologiques et Minières, Orléans

ABSTRACT

In a well, after an acoustic waveform has circulated through the surrounding porous media, the study of its alteration can help in evaluating their permeability.

The treatment of the acoustic compressional wave's first three cycles yields a unique parameter called I-c.

The recording of this I-c log all along any open hole interval is now possible by respecting some practical rules known by logging companies.

Large flows of fluid found in geothermal low-enthalpy operations have provided an opportunity to check the validity of this method.

Cumulative I-c derived permeability with depth ("EXAFLO" log) correlates with the flowmeter log, as examples will show.

Some new aspects of the theory underlying the I-c/permeability relationship have been developed and are described here.

INTRODUCTION

Geothermal resources are now recovered by fluids circulating through wells drilled down to favourable porous permeable reservoirs. Whatever the exact process used for circulation on the site and for the engineering requirements, the permeability values of the rocks crossed through have to be known by direct or indirect measurements. A direct permeability measurement can be made in the lab on a core taken from the subsurface. Even in the oversimplified case of an infinite continuous homogeneous bed the core measurement value is not always equal to the corresponding in situ value because full downhole conditions are difficult to reproduce in the lab. On the contrary if determined by well logging the in situ rock permeability measurements will be representative since they are made on radially continuous media. Even borehole effects on permeability may be evaluated.

Since well logging is performed at regular depth intervals in vertically heterogeneous media, the corresponding volume of investigation is also heterogeneous. But a permeability log will integrate vertically overlapping values whose continuous variations will then reflect actual permeability variations better than a discrete core measurement profile. Of course the direction along which the logging measurement is made will have to be specified.

A logging method suited for a permeability measurement will surely have to put the various saturating fluids and the matrix into measurable relative motion. To date neither electric, nor radioactivity nor nuclear magnetic resonance logs can create a noteworthy relative fluids-matrix motion. Among all other available logging methods, acoustics seems to be the most apt for creating and detecting these relative motions.

Production logging tools, such as the spinner flowmeter (in the high permeability range) and shale indicators such as the natural gamma ray log (in the low permeability range) will be useful calibrators for checking any valid permeability log.

OJECTIVE

We propose to study acoustic logs derived from body waves having traveled into the rocks around the borehole. Surface waves have an undetermined (if any) volume of investigation in the rock around the borehole and are, for that reason, kept outside the scope of our paper.

CURRENT ACOUSTIC LOGGING TOOLS

A pressure wave is regularly emitted in the borehole liquid mud. It propagates by refraction in the surrounding media. Pressure signals are then reemitted into the mud and detected.

P-wave velocity logging has been practised since ca.1950. Starting in 1962 research has been performed on the wavetrains obtained

with a number of tools. S-wave velocity logs are now currently run with long-spacing tools.

The transducers are either magnetostrictive scrolls or ceramic cylinders (1" to 3" diameter). The waveforms are received at a few feet from the transmitter. In view of the well radius (a few inches) and of the spacing length (a few feet), transducers may be considered as pinpoint devices. According to the transducer type, the emitted signal modal frequency is comprised between 10 and 30 kHz. The signal is recorded at about every half-foot of depth and digitized at least every 4 microseconds.

METHOD

The successive steps of our study will comprise :

1. A mathematical modeling of the signal, showing the importance of certain parameters,
2. A physical theory attempting to describe the actual permeable medium behaviour when traversed by an acoustic vibration,
3. A number of examples where logging vs. direct permeability comparisons are shown.

1. MATHEMATICAL MODEL

Spot acoustic probes are placed on the axis of a liquid-filled cylinder surrounded by an infinite elastic solid. However to make the model more realistic, the receiver may be, in the following equations, eccentered on the borehole side. Permeability occurrence in the medium will be modeled by open fractures with given apertures.

For this model complete formalism was developed by B. Conche(1) who quotes earlier literature on the topic(2).

The wave induced displacement $\vec{U}$ obeys the Navier equations. When $\vec{U}$ is written in terms of potential the wave equations are :

$$\Delta\Phi = \frac{1}{V_p^2} \cdot \frac{\partial^2\Phi}{\partial t^2}$$

with Φ = compression potential
V_p = P-wave velocity

$$\Delta\Psi = \frac{1}{V_s^2} \cdot \frac{\partial^2\Psi}{\partial t^2}$$

with Ψ = shear potential
V_s = S-wave velocity

In the Fourier domain (frequency, wavenumber) the cylindrical symmetry provides a simplification of these equations. Bessel functions can supply the analytical solutions to these equations. The source term is introduced as the P-wave direct propagation in the fluid, i.e. a particular solution.

Boundary conditions expressed on the circular wellbore help fix the constants in the solutions :

- radial stress and strain continuity,
- zero shear stress on the surface of the wellbore.

The transfer function simulating the rock is thus obtained analytically. When convolved with the source signal it will yield the synthetic seismogram.

Study of the P-wave received for a given source

The concept of a single peak pressure pulse (Dirac) as a source, is first considered. After such a peak has traveled in an attenuating medium, its response will be a typical wavelet decreasing with time, fig. 1.

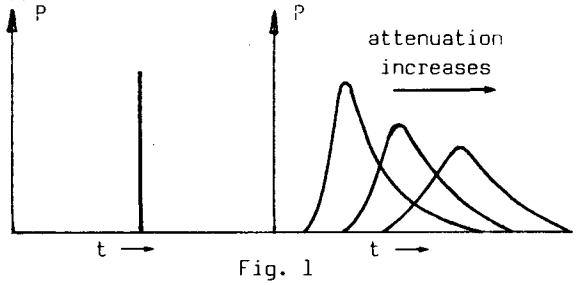

Fig. 1

Extension of this concept to any vibratory source signal focuses attention on the slope of the first amplitude. A plausible signature based on actual magnetostrictive scroll records will be found on fig. 2-26 and used in the rest of our model.

The effect of attenuation on the refracted P-wave is now the problem to be solved.

The parameter characterizing the P-wave signal must be chosen so that they are unaffected by the body wave interferences, i.e. picked up early enough in the first cycles of the P-wave.

We propose :

- the risetime (fig. 2-23), by definition it is the ratio of the first amplitude value over the slope at the inflexion point of the first rising branch of the signal,
- I-c index(3) (fig. 2-22), which is the ratio of the first two inflexion slopes with same polarity found on the P-wave.

These two parameters are apt to be altered by attenuation imposed on the signal, which in turn, is related, one way or another, to the permeability (if any) of the medium. The same parameters could be extracted from the S-wave, using special logging tools and processes (not treated here).

An attenuation-frequency relationship will now be imposed on the parameter calculation. The amplitude spectra will also be computed.

Results :

A Model with no intrinsic attenuation : see colunm 0 on the table I

B Model with attenuation. Here the attenuation is taken as an exponential function decreasing with the square of frequency.

The absorbed energy is modeled as a relative solid-fluid motion. The signal makes the solid drag the viscous fluid acting in VOIGT viscous-elastic model and governed by the DARCY's law.

For these signals the quality factor "Q" may be written as a function of the fracture equivalent aperture "l".

$$Q = 2\pi \frac{W}{\Delta W} = \frac{12\,\mu\,\rho_{solid}}{\rho^2_{liquid} \times l^2} \times \frac{1}{\omega}$$

For three different apertures of these fractures, the attenuated signals are represented on table I.

fracture aperture (in μ)	0	100	200	300
rise time (in μs)	6.6	7.4	11.2	16.3
I-c (dimensionless)	3.7	4.2	6.5	9.6
attenuation (fig)(2)		(40)	(43)	(46)
spectrum (fig)(2)	(27)	(41)	(44)	(47)
signal (fig)(2)	(26)	(42)	(45)	(48)

TABLE I

Both risetime and I-c increase with fracture apertures, i.e. with equivalent permeabilities.

A quite close model was used by Toksöz et al. (1984)(4) in which every factor, such as P-wave velocity and quality factors Q_p and Q_S were kept constant, but the S-wave velocity, i.e. the Poisson coefficient. For a Poisson coefficient varying from 0.22 to 0.37, I-c remains practically unchanged (6 to 7). This suggests that I-c for a given attenuation, (i.e. in the model for a given permeability) is largely independant of any lithology and porosity effects.

2. PHYSICAL THEORY

Porosity

A permeable medium always has a certain porosity though sometimes quite small ($\sim$ 0.001). If only made up of one-directional fractures the permeability will vary from very large in the fracture direction to almost nil in a perpendicular direction.

When the fractures have any direction or when the porosity is intergranular, the permeability value will be less affected by its direction.

A microscopic examination shows that even a so-called intergranular porosity is made up of voids of any shape. Their dimension ratios are rather high as in fractures. For the relative solid/fluids motion induced by acoustic signals, the intergranular porosity can thus be considered as an accumulation of random interconnected fractures.

Saturating fluids

Water is the basic fluid impregnating the whole porosity found in sediments. 95 % of this water is of meteoric origin. It is trapped in the sediments with a certain amount of atmospheric gases adsorbed on the matrix surface or dissolved in the water itself. This water reacts with the minerals making up the sediments. Depending on temperature, pressure and concentrations, the resulting connate water will reach an equilibrium. In some reservoirs oil and organic gases expelled from source rocks may displace the connate water but a fraction of it always remains in the porosity. For example a 4 to 17 % content of dissolved organic gases was found in the Paris basin geothermal reservoir porosity.

Among other gases found in the subsurface a special mention has to be made of argon and helium. For one thing Ar is trapped in connate water through atmospheric gases, but also because radiogenic processes continuously produce them from 40 K and U + Th. Now inert gases are less soluble in water than organic gases. H_2O-Ar concentration isotherms from 0 to 400 bars are represented in fig. 3. In the subsurface an additional solute content should lead us to estimate a still lower dissolved Ar fraction (see dotted curve 100°C). The cross-hatched region in fig. 3 is the one where liquid H_2O and gases coexist and where low-enthalpy geothermal reservoirs do occur.

Similar isotherms would be obtained for H_2O-He systems.

Experimental investigations of helium, argon and carbon in some natural gases

This study was performed on 39 samples of natural gases representing varying chemical composition and geological occurrences in the U.S.A. (1961)(5). Organic gases (CH^4, C^2H^6, CO^2) were found to represent from 50 to 98 % of the whole gas phases under surface conditions.

On figure 4 the volumetric concentrations of (He+Ar) are plotted vs. the concentration of total organic gases for the above-studied samples. Average result for about 20 geothermal Dogger reservoirs (France) obtained by Fouillac (1984)(6) was added. (He+Ar) content is found to increase regularly when organic gases content decreases.

Then in situ, at equilibrium, a free gas phase of 1 %, or more, in volume is to be expected in the connate water or in the mud-filtrate having invaded the drilled formations.

P-wave effect on the liquid-gas system in a porous medium

This free gas (bubbles or layers spread over the matrix surface) contributes to the attenuation of body waves traversing the formation. When a P-wave starting with a depression reaches a given depth in a porous formation, the gas-filled volume cannot increase if the surrounding uncompressible liquid cannot move, i.e. if there is no permeability at this depth.

On the contrary if there is a local permeability, the uncompressible liquid can move and the gas volume can increase. The greater the permeability, the more energy is absorbed from the P-wave for a given liquid of viscosity μ .

In view of the bubble or adsorbed layer size, the energy absorbed by the gas comes from the high frequency part of the signal spectrum. This intrinsic attenuation (A_i) adds up to the geometrical attenuation (A_g) :

$$\text{total attenuation} = (A_i).(A_g)$$

In the signal the positive pressure branch following immediately this first depression will tend to reduce the bubble, but the energy it has absorbed is not returned to the P-wave.

The second depression will now act from a somewhat different and weaker P-wave signal, cleared from a part of high-frequency, and the bubble size will not be so affected.

As the rock investigated volume and borehole section are the same in the two successive depressions, the geometrical attenuations (A_g) (independent of frequency) will be common for both cases.

This factor (A_g) covers the borehole effects (wellsize, mud-cake) and the solid-solid friction which varies with the lithology.

On the received signal the rates of depression are representative of the energy absorbed by attenuation. In forming the ratio I-c of both amplitude slopes, the effect of the geometrical attenuation is cancelled.

A single-valued relationship is linking I-c and permeability for a given liquid viscosity. We propose

$$\text{I-c} = \alpha \log \frac{Kv}{\mu} + \beta \qquad (1)$$

suggested, among others functions, by correlations with direct data.

Kv : being the permeability evaluated along the well bore axis direction,

α, β : constants attached to given tool and signal,

μ : the dynamic viscosity of the liquid phase.

As, in a well, the rock lithology and the borehole geometry are continuously varying with depth, the risetime parameter cannot be retained as a useful measurement of frequency dependent attenuation or permeability.

3. EXAMPLES

1. Two geothermal wells were drilled few miles apart by the B.R.G.M. (1982) through the Dogger formation in the Paris basin.

The reservoir was found in a limestone whose an interval of about 150 m thickness is represented on fig. 5.

Most of this interval is non-shaly and very porous ($20\ \% < \phi < 30\ \%$) as can be seen from the Neutron log. Core examination confirmed these properties. However only limited thickness intervals are actually water-producing as it can be inferred from the study of the spinner flowmeter log. The I-c log is showing some high values, i.e. some permeable intervals, but, at first glance, correlation with the flowmeter log is not evidently quantitative.

Cumulation of I-c derived permeability should yield a pseudo-flowmeter log, insofar as the reservoir pressure remains constant.

Here this cumulative permeability log (EXAFLO) is made from total depth up to casing shoe. For one of these wells, they will be found on fig. 5.

Correlation between both profiles is satisfactory. Permeability measurements derived from the flowmeter log may then confidently be used for calibrating the I-c log.

This calibration should prove valid for other I-c logs run with the same acoustic tool.

o
o o

The two following examples are relative to sand and shale formations.

Crouy 12 and Crouy 26 were drilled by Gaz de France (1982) through the aquifer sand of the Wealden formation (Paris basin) in view of extending an inderground gas storage. I-c log was run in both wells.

2. Crouy 26 (fig. 6). Over the 890-980 m interval I-c varies from 3 to 41. The histogram of I-c shows a number of modes which can be interpreted in the following way:

$3 < I\text{-}c < 10$ shale to shaly sands

$10 < I\text{-}c < 20$ clean sands

$22 < I\text{-}c < 41$ highly permeable coarse sands

Cumulative I-c (EXAFLO) singles out the upper part of the interval (890-923 m) as productive and/or injectable.

A similar interval is found from 942 to 950 m. These interpretations have been confirmed by tests. Flowmeter log was not run.

3. Crouy 12 (890-940 m). Direct permeability measurements are only known from plugs taken on recovered cores. Values spread from 1 to 10,000 millidarcy, fig. 7.

Apparently the upper part of this aquifer would be considered as highly favorable for gas injection. Now I-c log, run with the same tool as the one used for example (2) over the same formation, does not show values over 10, corresponding to a cut-off permeability in the example of Crouy 26.

Indeed CR-12 was eventually cased and the annulus was cemented, for further use as a surveillance well of the underground storage.

Starting in 1983, checks on gas content around CR-12 are regularly made by running of Gaz de France Neutron logs (fig. 7). To date no gas breakthrough was ever noticed within the investigated zone around CR-12. This fact does confirm that this sand-shale sequence is not permeable at CR-12 as I-c log had already shown it.

CONCLUSION

The first publication about I-c was made in 1978(3). As a permeability log derived from the computer treatment of acoustic waveforms, it was then used in geothermal wells in the Paris basin (1982). Its presentation is regularly improved and completed.

Mathematical models and physical theories are continuously adapted for better investigating the domain of this new logging method.

Large flows of fluid found in geothermal operations checked the validity of this method.

Low permeability shaly sands were correctly analysed.

For a given acoustic tool its calibration does not seem to vary with lithology or borehole variations.

REFERENCES

(1) CONCHE B., Apport des diagraphies dans l'identification de la fracturation, Mémoire IPG, Strasbourg, 1985.

(2) TSANG, RADER, Numerical evaluation of transient acoustic waveform due to a point source in a fluid-filled borehole, Geophysics, vol. 44, n° 10, october 1979.

(3) LEBRETON, SARDA, TROCQUEME, MORLIER, "Logging tests in porous media to evaluate the influence of their permeability on acoustic waveforms", SPWLA, El Paso, 1978.

(4) TOKSOZ, WILKENS, CHENG, Determination of shear wave velocity and attenuation from waveforms in low-velocity formation, M.I.T. (1984).

(5) ZARTMAN R.E., WASSERBURG G.J., REYNOLDS J.H., Journal of Geophysical Research vol. 66, n° 1, 1961.

(6) FOUILLAC C., GOYENECHE O., LOMBART R., SPITERI P., Hydrogéologie-Géologie de l'Ingénieur, n° 1, 1984.

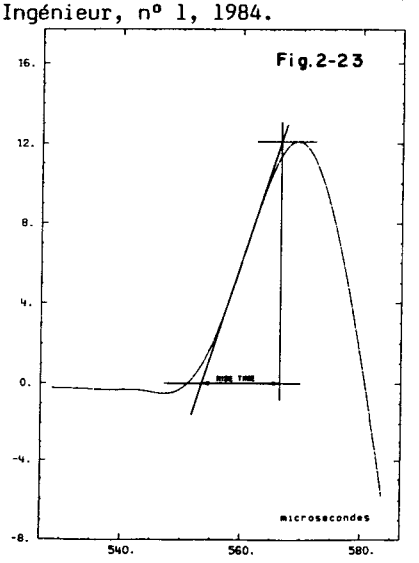

définition du " rise time " ou temps de montée : rapport de l'amplitude de la première crête sur la tangente au point d'inflexion de la première branche ascendante du signal

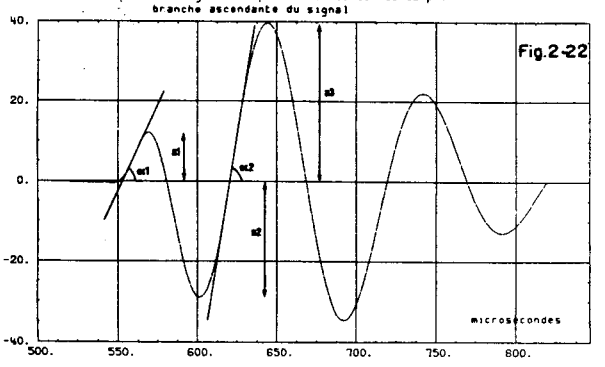

définition de l'indice ic :
- par les amplitudes (en valeurs absolues) : (a2+a3)/a1
- par les tangentes : Tang(alpha2)/Tang(alpha1)

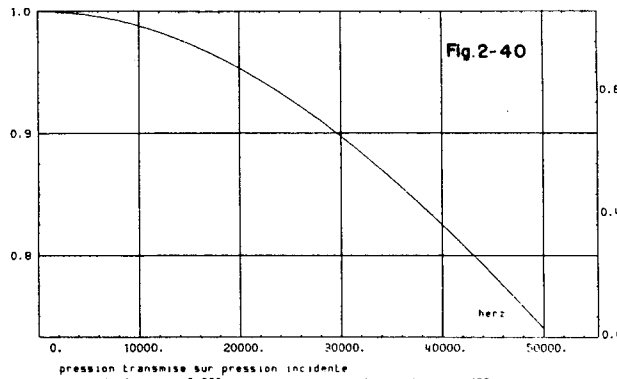

pression transmise sur pression incidente
rayon du forage = 0.080 m epaisseur de la fracture = 100. microns
d1=1050.kg/m3 vp1=1600.m/s d2=2600.kg/m3 vp2=5800.m/s vs2=3400.m/s

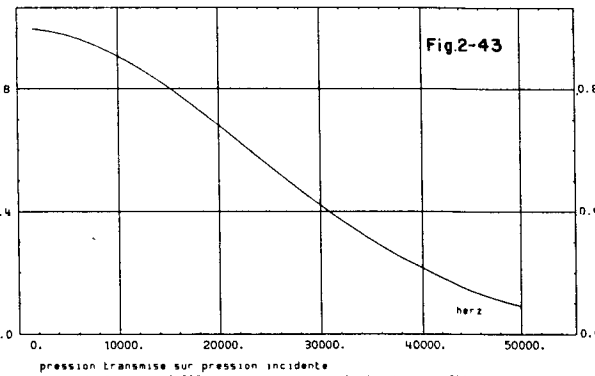

pression transmise sur pression incidente
rayon du forage = 0.080 m epaisseur de la fracture = 200. microns
d1=1050.kg/m3 vp1=1600.m/s d2=2600.kg/m3 vp2=5800.m/s vs2=3400.m/s

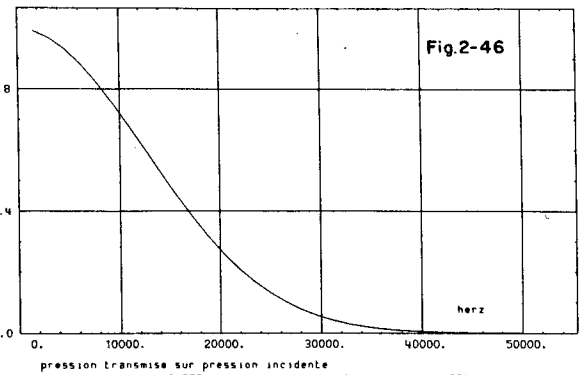

pression transmise sur pression incidente
rayon du forage = 0.080 m epaisseur de la fracture = 300. microns
d1=1050.kg/m3 vp1=1600.m/s d2=2600.kg/m3 vp2=5800.m/s vs2=3400.m/s

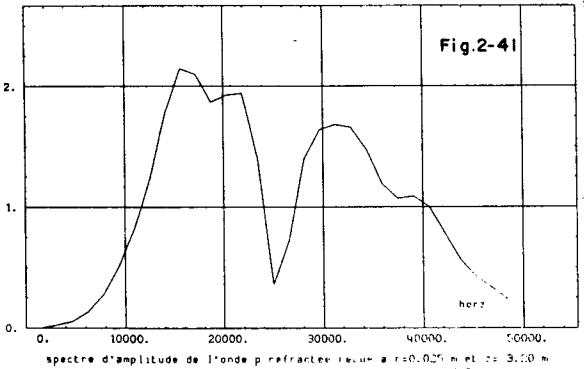

spectre d'amplitude de l'onde p refractee recue a r=0.025 m et z= 3.20 m
rayon du forage = 0.080 m epaisseur de la fracture = 100. microns
d1=1050.kg/m3 vp1=1600.m/s d2=2600.kg/m3 vp2=5800.m/s vs2=3400.m/s

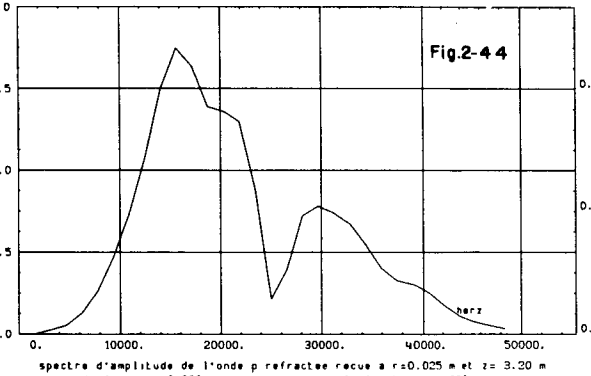

spectre d'amplitude de l'onde p refractee recue a r=0.025 m et z= 3.20 m
rayon du forage = 0.080 m epaisseur de la fracture = 200. microns
d1=1050.kg/m3 vp1=1600.m/s d2=2600.kg/m3 vp2=5800.m/s vs2=3400.m/s

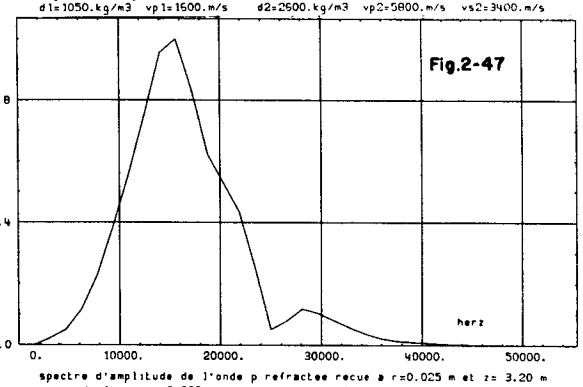

spectre d'amplitude de l'onde p refractee recue a r=0.025 m et z= 3.20 m
rayon du forage = 0.080 m epaisseur de la fracture = 300. microns
d1=1050.kg/m3 vp1=1600.m/s d2=2600.kg/m3 vp2=5800.m/s vs2=3400.m/s

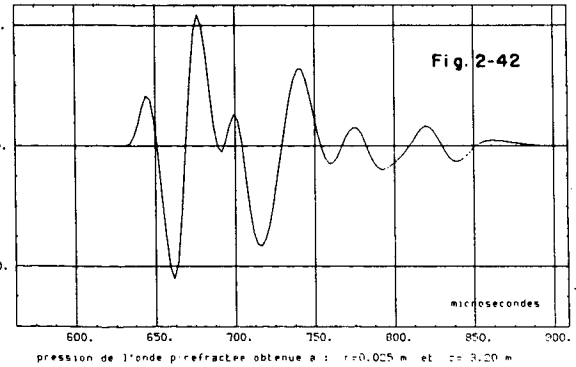

pression de l'onde p refractee obtenue a : r=0.025 m et z= 3.20 m
rayon du forage = 0.080 m epaisseur de la fracture = 100. microns
d1=1050.kg/m3 vp1=1600.m/s d2=2600.kg/m3 vp2=5800.m/s vs2=3400.m/s
ic(pics)= 5.3 ic(tangentes)= 4.2 rise time= 7.4 microsecondes

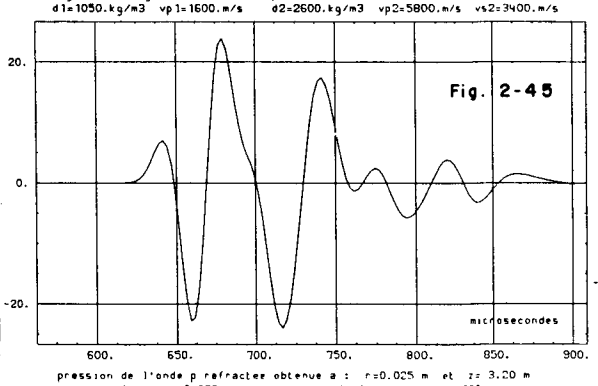

pression de l'onde p refractee obtenue a : r=0.025 m et z= 3.20 m
rayon du forage = 0.080 m epaisseur de la fracture = 200. microns
d1=1050.kg/m3 vp1=1600.m/s d2=2600.kg/m3 vp2=5800.m/s vs2=3400.m/s
ic(pics)= 6.7 ic(tangentes)= 6.5 rise time=11.2 microsecondes

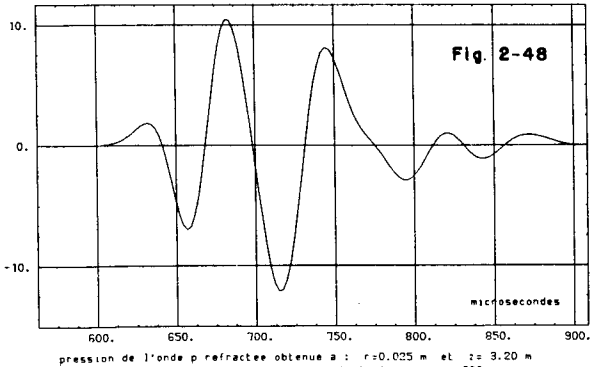

pression de l'onde p refractee obtenue a : r=0.025 m et z= 3.20 m
rayon du forage = 0.080 m epaisseur de la fracture = 300. microns
d1=1050.kg/m3 vp1=1600.m/s d2=2600.kg/m3 vp2=5800.m/s vs2=3400.m/s
ic(pics)= 9.4 ic(tangentes)= 9.6 rise time=16.3 microsecondes

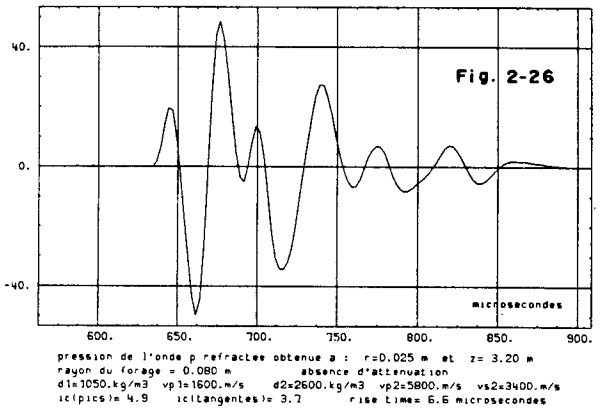

pression de l'onde p refractee obtenue a : r=0.025 m et z= 3.20 m
rayon du forage = 0.080 m absence d'attenuation
d1=1050.kg/m3 vp1=1600.m/s d2=2600.kg/m3 vp2=5800.m/s vs2=3400.m/s
ic(pics)= 4.9 ic(tangentes)= 3.7 rise time= 6.6 microsecondes

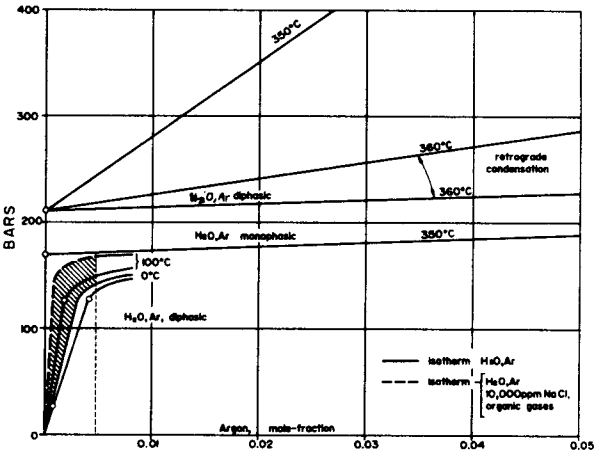

Fig:3- after International Union of Pure and Applied Chemistry Solubility data Series.

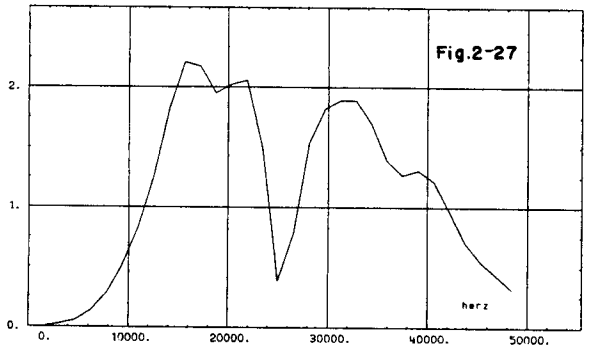

spectre d'amplitude de l'onde p refractee recue a r=0.025 m et z= 3.20 m
rayon du forage = 0.080 m absence d'attenuation
d1=1050.kg/m3 vp1=1600.m/s d2=2600.kg/m3 vp2=5800.m/s vs2=3400.m/s

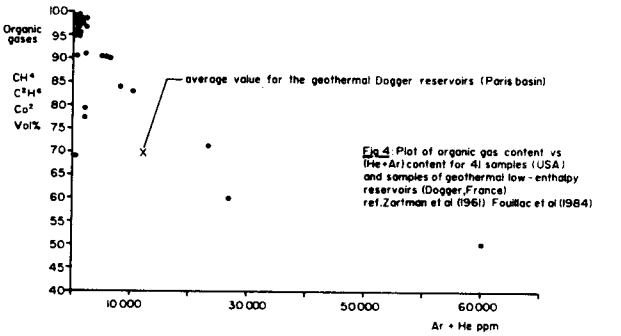

Fig.4 Plot of organic gas content vs (He+Ar) content for 41 samples (USA) and samples of geothermal low-enthalpy reservoirs (Dogger, France) ref. Zartman et al (1961) Fouillac et al (1984)

Fig5: AULNAY - SOUS - BOIS

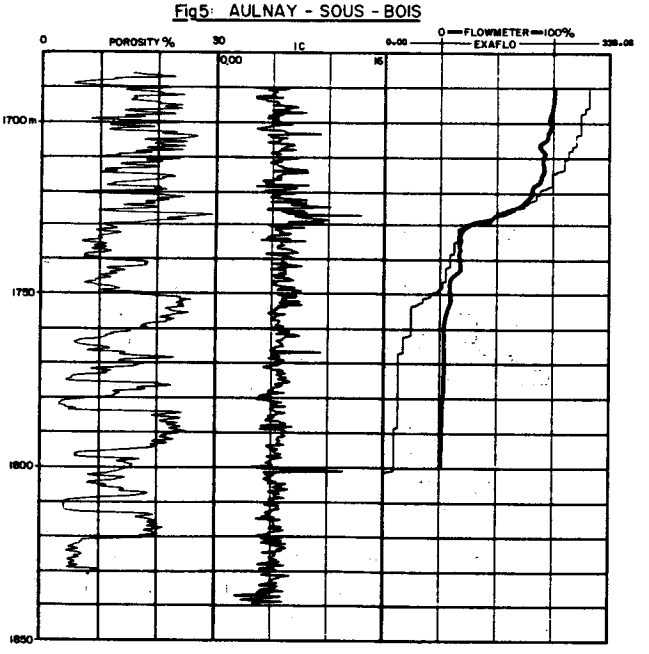

PUITS CR-26 (Gaz de France)

INDICE IC EXAFLO

Fig. 6

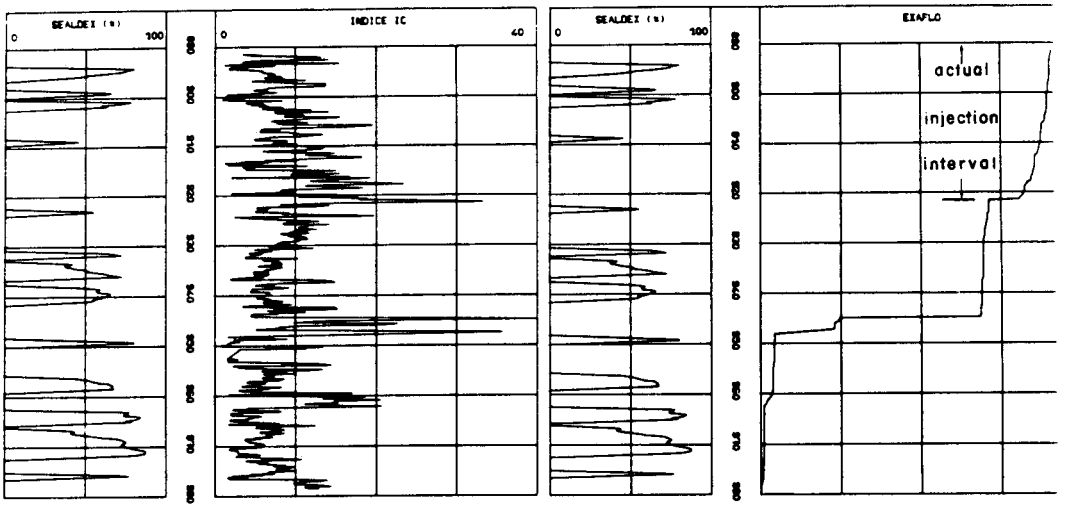

CROUY 12 (GAZ DE FRANCE)

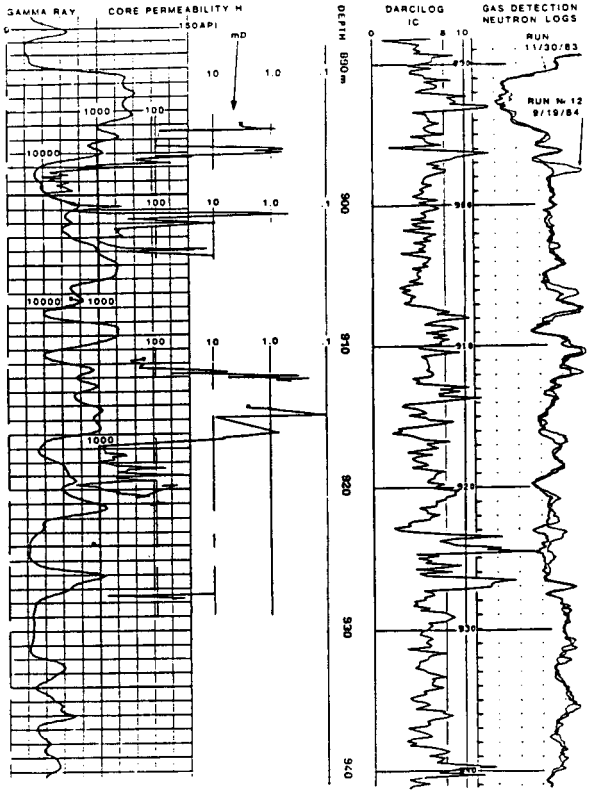

Fig. 7 - NO SIGNIFICANT GAS CONTENT IS DETECTED AROUND THIS SURVEILLANCE WELL DRILLED TROUGH AN UNDERGROUND GAS STORAGE